7. ANKARA INTERNATIONAL AEROSPACE CONFERENCE
11-13 September 2013 - METU, Ankara TURKEY

AIAC-2013-045

CREEP LIFE IMPROVEMENT BY REDESIGNING OF A TURBINE STAGE

Cihat Akın[1] Tolga Yasa[2]
TUSAS Engine Industries
Eskisehir, Turkey

ABSTRACT

Creep life is one of the most important design criterion in a gas turbine. In order to have competitive engine life, the stresses and the metal temperatures should remain at acceptable levels. The turbine of a mini turbojet engine is investigated in terms of creep life. The significant life enhancement is achieved by redesigning of the turbine stage. The aerodynamic performance of both designs are compared by means of Reynolds averaged Navier-Stokes simulations. The stress distribution is analyzed by finite elements methods. The blade critical stress values are reduced by 37% with the new design while increasing the creep life of the component. The results are verified by engine testing based on fuel consumption rate.

INTRODUCTION

Aero-engine designers aim to increase durability of the engines in order to reduce the operational costs. In turbomachinery, the hot-section components are life limiting elements due to harsh working conditions. The gas temperature after the combustion chamber is extremely high and it is often beyond the melting point of the materials. Thus, the turbine components are subjected to temperature related problems such as creep, oxidation, and thermal stresses. Failure mechanism at turbine section depends on the operating conditions. Mechanical fatigue is usually the dominant failure mechanism up to gas temperature of 800 °C. At higher temperatures, up to 1000 °C, creep oxidation and thermal fatigue (acting alone or together) usually cause the failure. In the intermediate temperature range, i.e. 800 to 1000 °C, any of the failure mechanism described cause the engine break down [Naeem, 2009].

The creep behavior is usually expressed by well-known Larson-Miller parameter [Larson and Miller, 1952]. This parameter links the applied stress value, operating time and material temperature. Different mechanisms cause creep in the micro-structure of the materials. The dislocation creep occurs when a dislocation come upon a blockage. Then, it makes a climbing motion by the aid of the thermal activation [Ejaz et al., 2011]. At high temperatures and slow deformation speed, grain slips over the boundaries, called as the “grain boundary sliding creep”. Raj and Ashby made a detailed research on the physical mechanism of the problem at non-planar grain boundary [Raj and Ashby, 1971]. The creep mechanism is also investigated on two dimensional model polycrystal [Mor et al., 1998]. The paper formulates the deformation rate due to creep failure.

There are basic creep life prediction methods for the turbine blade design. One of the early prediction methods is developed based on the blade temperature distribution, material data and visco-plastic finite element model [Dambrine et al. 1988]. The microstructure change of the in service turbine blades are investigated and a simple remaining life prediction method is obtained by Persson and Persson [Persson and Persson, 1993]. Jianping et al. compared different creep life prediction models using a stream turbine case. They concluded that nonlinear continuum damage model gives the most accurate results [JianPing et al., 2006]. An accurate exhaustion of strain energy density based damaged model is presented for the creep life assessment, [Jelwan et al., 2013]. Beside the theoretical models, a full scale turbine blade is tested for creep by Yan and Nie. A life prediction model is then generated using experimental data which was found to be in good agreement with the field

[1] Aerodynamic Engineer, Email: cihat.akin@tei.com.tr
[2] Turbine Component Design Leader, Email: tolga.yasa@tei.com.tr

data [Yan and Nie, 2008]. In order to reduce the uncertainty of the life prediction method, finite element methods are used either after the aerodynamic designing process [Kumar, et al. 2012] or by coupling it to the optimization process of the design [Arabnia et al. 2011].

The creep life of the blades (time to rupture, time to strain) is controlled by design parameters such as flow-path dimensions, the rotational speed and the taper ratio (A_{tip}/A_{hub}) [Mattingley et al. 2002]. The blade hub mechanical loading (AN^2) is an important parameter to define the design space due to lifing limits [Stricker, 1998]. The design based structural improvement studies are commonly targeting either restacking of the 2D sections [DiCristoforo et al. 2004] or local improvements such as trailing edge thickening [Gill, 1995]. These actions are mostly enhancing local areas of the blade to overcome stress concentrations. Since the temperature dominates the creep mechanism, the blade temperatures must be controlled properly during the design either by cooling or choosing the right degree of reaction [Rodgers, 1976]. In case of significant life improvement, the engine may subject to radical design changes such as annulus area.

In the current study, the turbine section of a mini turbojet engine is redesigned. The design parameters of the new section are arranged in such a way that the turbine lifespan is increased without changing the material. The turbine flow-path is changed respecting the interfaces. The turbine metal temperature is reduced by manupulating the reaction parameter. The aerodynamic performance of the new design is compared with the previous one. Besides the numerical studies, the performances of both turbines are compared based on the engine test data. The life of the turbine module is increased by better controlling of the design process. The new crep life is predicted to be 18 times better than the previous design.

TURBINE DESCRIPTION

Initial Turbine Stage (model 1)

Initial turbine's design conditions are listed in Table 1. The main design constraint is the outlet swirl of the turbine. The turbine outlet must be axial in order to not lose the engine thrust. The turbine mean line reaction is kept at 0.44. The design is subject to an AN^2 value of nearly 49 million.

Table 1. *Model 1 Turbine design conditions*

Pressure ratio	2
Flow factor, V_x/U	0.44
Stage loading, $\Delta H/U^2$	1.17
Spesifific work, $\Delta H/T$	162.4 J/kg/K
Reaction	0.44
AN^2	49.2 million

The blade-to-blade view of the mid-section is also depicted in Figure 1. The turbine consists of 19 vanes of aspect ratio 1.16 with the exit absolute Mach number of 0.81 and 23 blades of aspect ratio 1.84 with the relative exit Mach number of 0.77 at the mid-span. The rotor turning is about 84 degrees. Mid-span rotor inlet relative total temperature is 1160 K. Some of the geometrical details about the airfoils are listed in Table 2. The all angular informations are normilized by the stator stagger angle.

Table 2. *Model 1 mid-span blade geometry*

	Stator	Rotor
Pitch to chord ratio	0.795	0.98
TE Wedge angle	6.5	9.2
Inlet metal angle	0	19.8
Outlet metal angle	68.9	64
Stagger	45	39.4

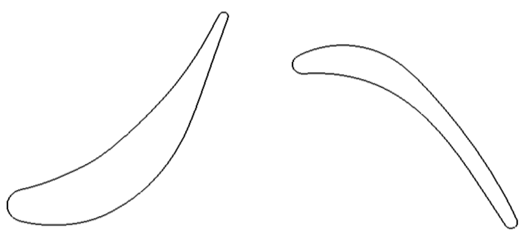

Figure 1. *Model 1 mid-span blade-to-blade view*

New Turbine Stage (model 2)

Model 2 turbine design conditions are listed in Table 3. In the new design the hub stress is significantly reduced (AN^2=42 million) by reducing the annulus area.

Table 3. *Model 2 turbine design conditions*

Pressure ratio	2.02
Flow factor, V_x/U	0.61
Stage loading, $\Delta H/U^2$	1.32
Spesifific work, $\Delta H/T$	164.8 J/kg/K
Reaction	0.38
AN^2	41.7 million

The new airfoils are shown in Figure 2. The new turbine has lower number of vanes (17) in the stator but the number of rotor blades is slightly increased (24). Similar to model 1, the flow is kept subsonic from inlet to outlet of the stage. The lower degree of reaction helps to reduce the relative gas temperature (1103 K) compared to the initial turbine stage. Once the reaction is lower the turbine loading is increased which also cause more effort on the airfoil design. More detail about the geometry is given in Table 4. The all angular informations are normilized by the stator stagger angle of the model 1.

Table 4. *Model 2 mid-span blade geometry*

	Stator	Rotor
Pitch to chord ratio	0.79	0.81
TE Wedge angle	6	5
Inlet metal angle	0	27.3
Outlet metal angle	65.3	53.8
Stagger	45	33

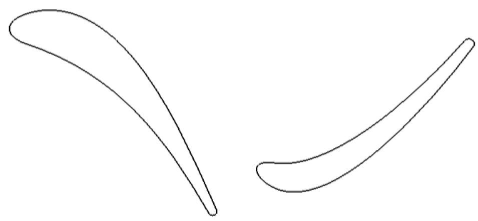

Figure 2. Model 2 mid span vane and blade

NUMERICAL METHODS

Design Approach

The Model 1 is designed by using commercial software package in the past. On the other hand, the new turbine is designed by using new in-house design codes. The redesigned turbine should meet the existing cycle requirements of the engine while achieving creep life improvement, performance improvement and weight reduction. Temperature distribution has been lowered by the manipulation of the reaction parameter since cooling application is not a conventional approach for such turbine inlet total temperature. The stress level is lowered mainly by the reduction of the AN^2 parameter. Since the compressor of the engine remains unchanged in the new design, the rotational speed is fixed. Therefore, the annulus area needs to be decreased in order to reduce the stress levels.

The mean line design of the turbine has been performed by using TEI in-house code “TEI-TurbM”. Then, the meridional design is performed by giving a special radial work distribution at the stator outlet flow. The work distribution is controlled easily by using another in-house code namely, “TEI-TurbR”. The radial work distribution is selected in such a way that the turbine outlet is axial and the hub reaction still remains above zero. Both design codes are recently developed at TEI in order to increase design flexibility and better control of design parameter. Finally, the blade geometries are obtained by using commercial codes.

Both designs have their unique exhaust nozzles that have sonic conditions while supplying the designed back-pressure to turbines (see Figure 8). Furthermore, nozzle design has been taken as a part of the turbine-redesigning process and the CFD models include nozzle geometry together with the turbine stage.

Aerodynamic Analysis

The computation has been performed by using a time marching RANS equations based 3D solver. The domain has been constructed by using structural H-O type mesh. Number of grid points is 1.2 million for the stator and 1.7 million for the rotor. Spalart-Allmaras [Deck et.al.,2002] model was used for the turbulent viscosity computation. The mesh of the model is depicted in Figure 3.

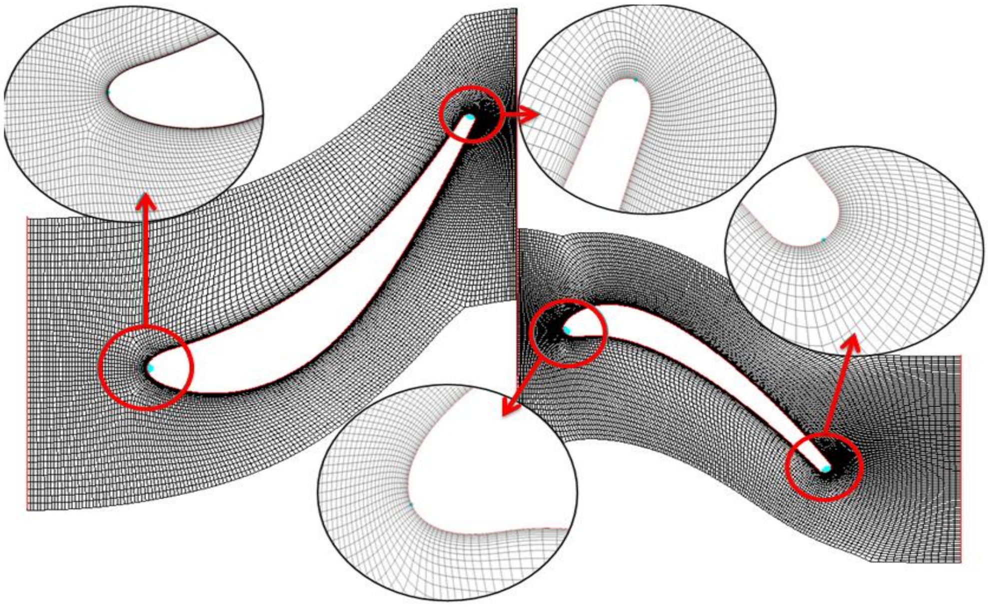

Figure 3. Computational domain and mesh topology

Boundary conditions have been imposed using the combustion chamber outlet total conditions in order to mimic the actual case. The turbine inlet total temperature (T_{t4}) and total pressure (P_{t4}) radial profiles that has been used in the calculation is given in Figure 4. The outlet boundary condition is set by the average static pressure value.

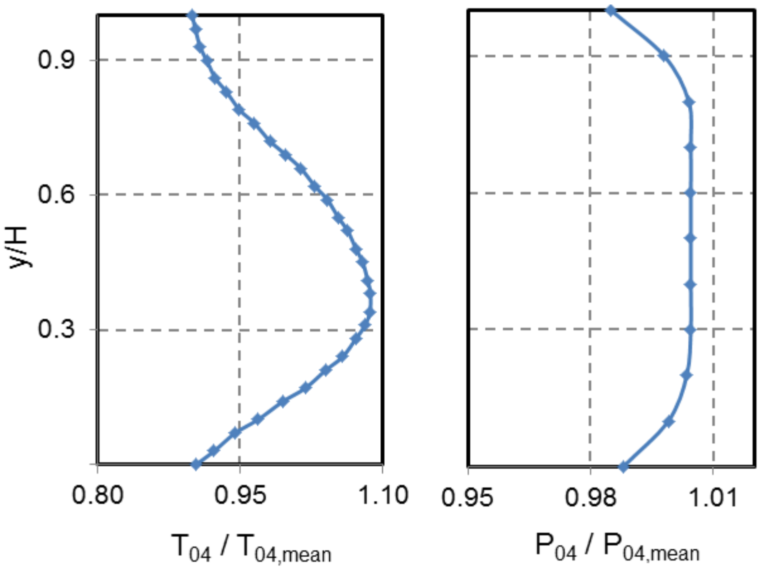

Figure 4. Turbine inlet total temperature and pressure profiles

Structural Analysis

The structural analysis has been conducted by commercial finite element software. The blade is modeled together with the disk assembly. The rotor is assumed periodic so only one blade is modeled (Figure 5). The mesh generation is done by using Solid95/Tet type meshing. In the final model around 10000 nodes and 70000 elements are generated. The model is axially and tangentially fixed from axial contact surfaces to the bearing inner race. All analysis has been performed at design rotational speed. No maneuver loads are included and any contact face is defined in the analysis.

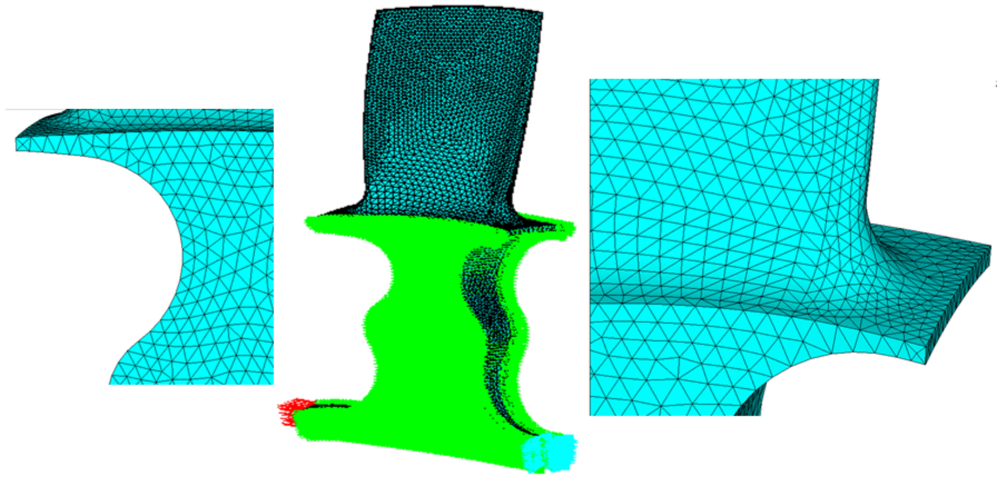

Figure 5. FEM model of the rotor

The temperature distribution is a very critical issue for the analysis. Commercial software is used to derive the temperature distributions on the solid bodies. It is specifically developed for turbomachinery applications. The combustion chamber outlet temperature distribution is used as boundary condition in order to have more realistic results. The results are shown in Figure 6. A unique mesh is used both for the thermal and the finite element models. Therefore, the surface temperatures are directly used in the structural analysis. The thermal validation test has been done in order to validate the solution.

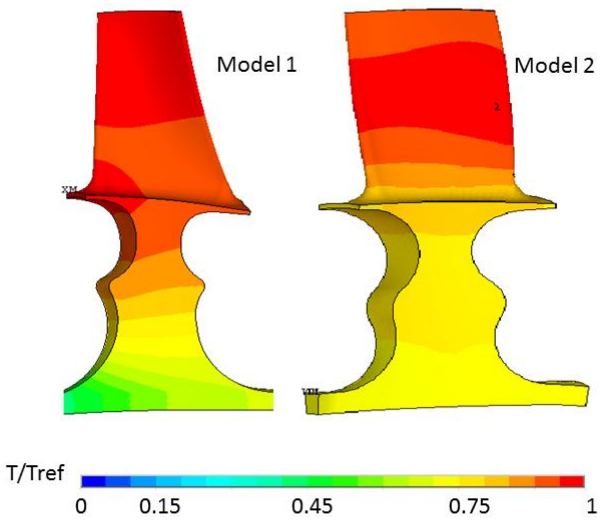

Figure 6. Temperature distribution of the both model

RESULTS and DISCUSSIONS

The creep life has been improved by reducing the blade stress via changing the flow-path. Lowering the mean radius causes an increase on axial velocities. It requires a very careful designing of the blade since the local velocity peaks result in local flow separations. The elliptical leading edges are employed in the new turbine design in order to alter such a problem.

The blade is leaned 1.5 degrees and swept -0.5 degrees to reduce the hub section pressure side bending stresses. Positive leaning results as an increase of tip loading which is not desirable due to the tip vortex. Therefore, the tip section turning has been lowered to compensate that effect [Beer, 2008]. Moreover, the hub reaction is reduced after the lean operation. Lower reaction is very critical for the off-design performance of the turbine so the hub section is redesigned in order to keep the reaction level at an acceptable range.

The third modification has been done on the vane outlet angle. It has been lowered to increase the mass flow capacity of the flow-path. The aspect ratios of both vane and blade have been chosen lower than the previous design as suggested by Lethander [Lethander, 2003]. All structural improvements result in a lower blade turning hence a lower work. In order to overcome the work loss the pressure ratio and the blade number has been modified.

Flow Field Analysis

The isentropic Mach number distributions of both designs are shown in Figure 7. Both models have a rapid acceleration on the leading edge of the airfoil due to the high curvature. The flow accelerates smoothly up to the throat of the vane (Figure 7-a). The new vane has more loading at the front part (up to throat). Hence the velocity peak at the throat is reduced in the new design. Additionally, the deceleration along the unguided section of the blade is decreased in the new design. Both effects increase the performance of the vane and lower the pressure losses. The design strategy is completely changed in the rotor (Figure 7-b). The previous design has a more mid-loaded blade whereas in the new design the blades are more front-loaded. The new strategy allows work extraction in early stage hence the metal temperature is reduced at the rear part of the blade. Lower metal temperature results in a better creep performance.

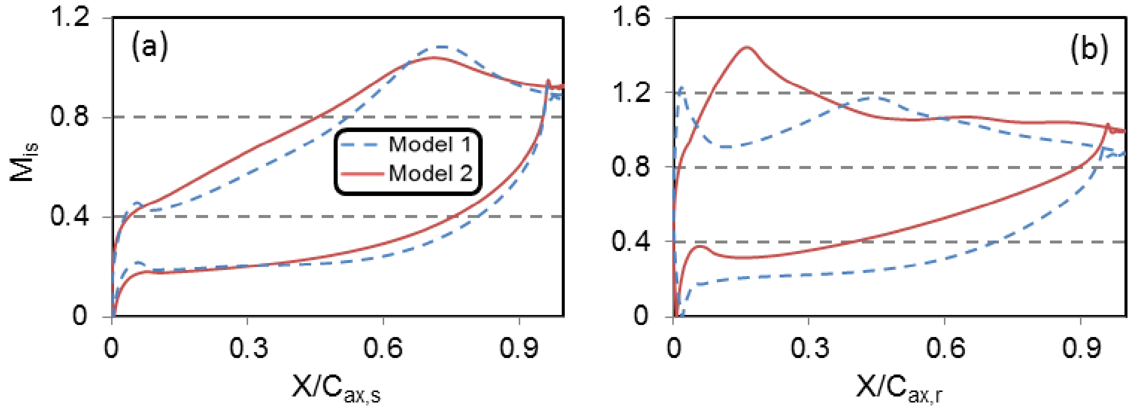

Figure 7. Isentropic Mach number distribution over the mid-span a) vane b) blade

The outlet flow fields of both turbines are compared in Figure 8 at 15% rotor axial chord downstream of the rotor trailing edge. The turbine outlet absolute swirl angle is depicted in Figure 8-a. The new model has more swirl angle than the previous design. However the change of swirl does not have a significant effect on the engine thrust. The absolute total pressure values are also given in Figure 8-b. Although the new design is more loaded than the previous one the total pressure at the stage outlet is higher up to 65% of the blade height. It indicates that the new turbine has lower aerodynamic losses hence a better performance.

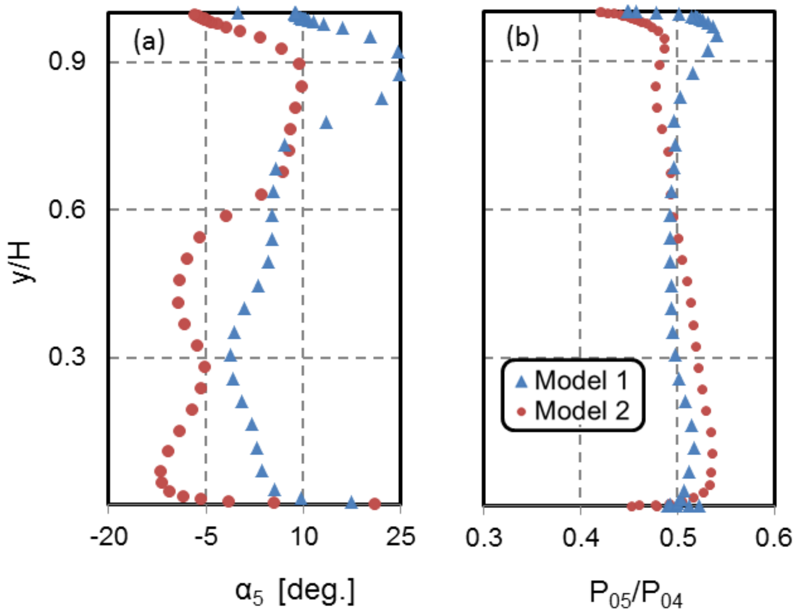

Figure 8. Stage outlet radial distributions a) absolute swirl angle, b) Non-dimensional total pressure

Both turbines are tested in the engine test-bed of TEI. The fuel rate, engine thrust and rotational speed data are collected during a typical test. The comparison is shown in Figure 9. The fuel consumption is presented in terms of specific fuel consumption (SFC). All results are normalized by using design target values. The SFC is an important figure of turbine performance as long as performances of the other components remain the same. The engine configuration (compressor and combustion chamber) is kept unchanged in both tests. Only the turbine and the exhaust nozzle are changed in engine. The thrust rating is presented in Figure 9-b. The similar thrust levels ensure the engine performance. The new turbine performed better at off-design conditions. Close to the design points, both turbines have similar characteristics. The tip clearances are also monitored regularly for both designs.

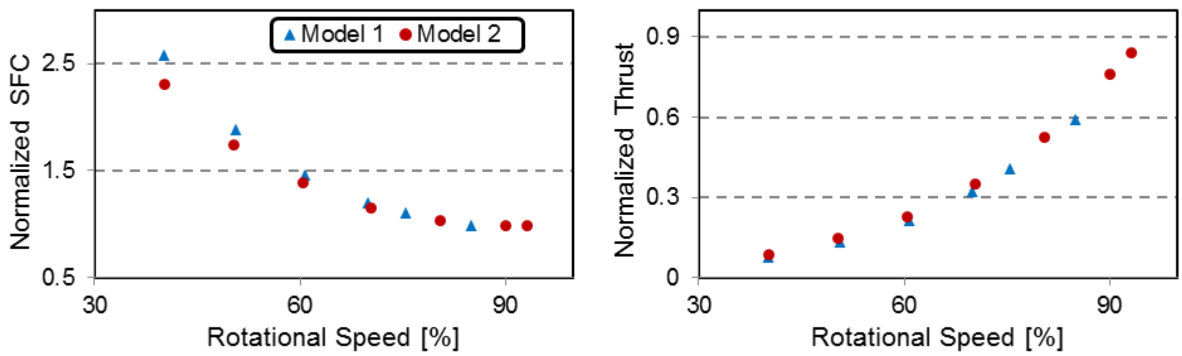

Figure 9. Engine test results of both turbines a) fuel consumptions b) thrust rating

Structural Improvement

The rotor integrity has been analyzed by comparing the stress levels. The results are plotted in Figure 10. The maximum tensile stress is obtained at hub region as expected. The new design has 37% lower stress in the critical region. The disk bore stress is also significantly reduced mainly due to the lower centrifugal blade loadings.

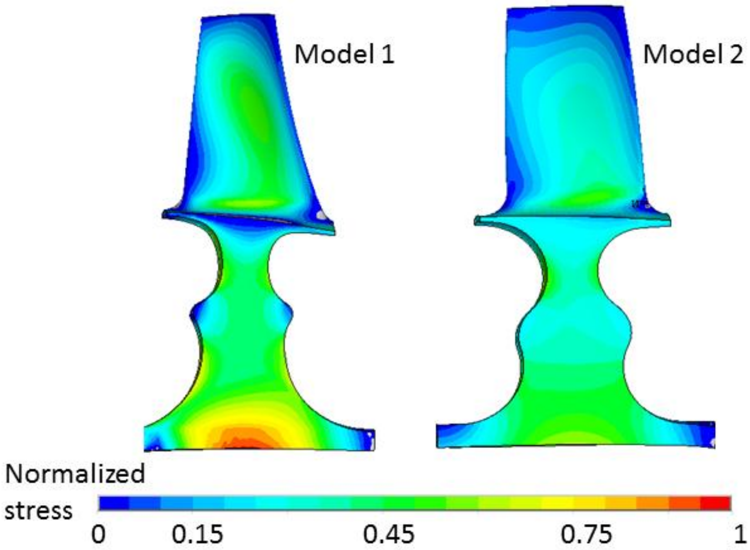

Figure 10. Rotor stress levels

The creep life of both designs is investigated around the mean radius region. Figure 11 shows the estimated creep life of each rotor. There is a significant improvement on the creep performance with the new design. The improvements mainly come from lower metal temperatures and lower stress concentrations.

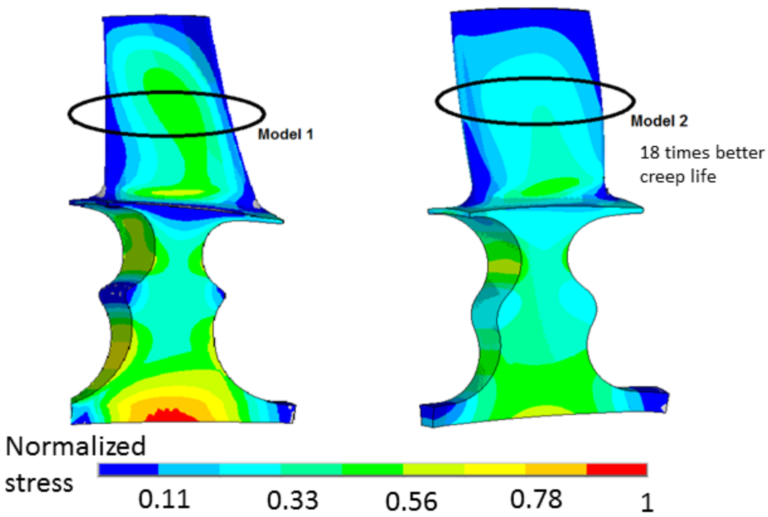

Figure 11. Rotor creep life estimation

The creep performance of both designs has been investigated experimentally by means of engine tests. A typical test cycle covers three minutes stop at several rotational speeds (idle, 50%, 60%, 70%, 80%, 90% of the design speed). The total run time is usually about 25 minutes. The maximum speed is determined when the gas temperature at the exhaust (EGT) reaches the design limit. After each run the turbine tip clearance is measured at four peripheral locations while the engine is not running.

The initial turbine runs up to 80% of the design speed whereas the new design goes up to 90% of the design speed for the same EGT limits during a typical test cycle. The blade deformation is observed after about five hours of running with the initial design. On the other hand, the new turbine runs more than thirteen hours without any physical change. The results also proof clearly the structural improvements.

CONCLUSION

The creep performances of two turbine designs have been investigated by using numerical tools. The previous turbine is found to be very vulnerable to the creep. The creep performance of the turbine has been improved by redesigning of the stage. The turbine flow-path is moved to a lower radius in order to lower the blade stress levels due to the centrifugal forces. Additionally, a better control of centrifugal forces is obtained when the blade is lean and swept. Finally the hub stresses are lowered by 37% and a significant increase on the creep performance is reached. The engine test also supports the numerical findings. The low work output of the new turbine is compensated by increasing the pressure ratio of the stage. The aerodynamic performance of the new design is verified by numerical simulations and the engine tests.

ACKNOWLEDGEMENT

The authors gratefully acknowledge the financial support of the “TUBITAK TEYDEB” programme.

References

Arabnia, M., Sivashanmugam, V.K., Ghaly, W., 2011, “Optimization of an axial turbine stage for aerodynamic inlet blockage”, ASME Paper, GT2011-46757.

Beer, W., 2008, “Optimisation of a compound lean turbine blade in a linear cascade”, Ph.D Thesis, Vienna University of Technology.

Dambrine, B., Mascarell, J.P., 1988, “Designing turbine blades for fatigue and creep”, Defence Science Journal, Vol.38, No.4, pp 413-430

Deck, S., Duveau, P., d’Espiney, P.,Guillen P., 2002, “Development and application of Spalart-Allmaras one equation turbulence model to three-dimensional supersonic complex configurations”, Aerospace Science and Technology, Volume 6, Issue 3, pp. 171–183

DiCristoforo, P.E, Elledge, M., 2004, “Stress redistribution for increased creep life in the GE MS6001 B second-stage blade”, Journal of engineering for gas turbines and power, Vol.126, issue 1 pp.127-130.

Ejaz, N., Qureshi, I.N., Rizvi, S.A., 2011,“Creep Failure of Low Pressure Turbine Blade of an Aircraft Engine”, Engineering Failure Analysis, Volume 18, Issue 6, pp. 1407–1414

Eno, D.R., Young, G.A, Sham,T.-L. 2008, “A unified view of engineering creep parameters”, In: ASME, *Pressure vessels and piping division conference*. Chicago, Illinois.

Gill, J.E., 1995, “*Uprate options for the MS900A Heavy-Duty gas turbine”,* New York: GE Power Systems, GER-3928A.

Ginter, T., Bouvay, T., 2006, “Uprate options for the MS7001 Heavy-Duty gas turbine*”,* Atlanta: GE Energy, GER-3808C.

Jelwan J., Chowdhury M., Pearce G., 2013, “Design for creep: A critical examination of some methods”, Engineering Failure Analysis, Volume 27, pp. 350–372

Jianping J., Guang M., Yi S., Songbo, X., 2006, “A Continuum Damage Mechanics Model on Creep Rupture Life Assessment of a Steam Turbine Rotor”, Journal of Engineering for Gas Turbines and Power, Vol. 128, Issue 6, pp. 173-177

Kumar, S.M.S., Manju, M., Raghavendra, S., 2012. “Creep life prediction of steam turbine blade using finite element method”, International Journal of Advanced Engineering Research and Studies*,* 1(2), pp.95-98.

Larson F.R. and Miller J., 1952, ”A Time-Temperature Relationship for Rupture and Creep Stresses”, Trans. ASME, vol. 74, pp. 765−775.

Lethander, A.T., 2003. “Assesmentof a leading edge fillet for decreasing vane endwall temperatures in a gas turbine engine”*,* Ph.D Thesis, Virginia Polytechnic Institute and State University

Mattingly, J.D., Heiser W.H., Pratt, D.T., 2002. “Aircraft engine design”, 2nd edition, Virginia, American Institute of Aeronautics and Astronautics, Inc.

Mor T., Onaka S., Wakashima K., 1998, ”Role of grain-boundary sliding in diffusional creep of polycrystals”, Journal of Applied Physics, Volume 83, Issue 12, Muhammad Naeem, 2009, “Implication of Day Temperature Variation for an Aero-Engine’s HP Turbine Blade’s Creep Life-Consumption”, Aerospace Science and Technology, Volume 13, Issue 1, pp. 27–35

Persson C. and Persson P. O., 1993, “Evaluation of service-induced damage and restoration of cast turbine blades”, Journal of Materials Engineering and Performance, Volume 2, Issue 4, pp 565-569

Raj R., Ashby M. F., 1971, “On grain boundary sliding and diffusional creep”, Metallurgical Transactions, Volume 2, Issue 4, pp. 1113-1127

Rodgers, C., 1976. “Advanced radial inflow turbine rotor program – design and dynamic testing”, *Technical report*, NASA

Stricker, J.M., 1998, “The gas turbine engine conceptual design process – an integrated approach”, RTO-AVT Symposium, *Design principles and methods for aircraft gas turbine engines.* Toulouse, France.

Yan XJ. and Nie JX., 2008, “Creep-Fatigue Tests on Full Scale Directionally Solidified Turbine Blades”, Journal of Engineering for Gas Turbines and Power, Vol. 130, Issue 4, pp.

AUTHOR ANSWER TO THE REVIEW OF PAPER AIAC-2013-045

OVERALL COMMENTS

The authors gratefully acknowledge the reviewers for their effort spent in the reviewing process. The detailed comments and suggestions have helped to improve the overall paper quality. A thorough revision has been made with the aim to accomplish all the required changes, to improve the readability and weak points of the paper. All the reviewers' comments and questions have been addressed and detailed answers are provided in the following. The original reviewer comments have been reported in *red and italic fonts*. The author answer is reported in **black**. New text added to the draft manuscript or original text that has been modified is reported in blue.

REPLY TO REVIEWER 02

(1) Why is the creep life comparison performed using only the data near the mid-span region rather than using the all available surface data?

The creep life comparison has been performed using the data over the whole blade including the platform and the disk. Due to inlet RTDF profile and temperature sensitivity of the creep life, although the maximum tensile stress location is at the hub, the critical-life section of the blade is around 40-60% span. Thus, the mean section creep life evaluation is pointed out in the paper.

(2) Swirl amount seems to have increased (Figure 8 left, red dots) but this seems to be not affecting the performance? What is the reason?

The stage outlet absolute swirl angle was about 5 degrees in the first design. The second model's swirl is around -8 degrees. Absolute increase of the swirl is about 3-4 degrees. Therefore the axial velocity components only changes by 0.24%. Additionally, the nozzle is redesigned in order to compansate the variation of the turbine exit conditions.

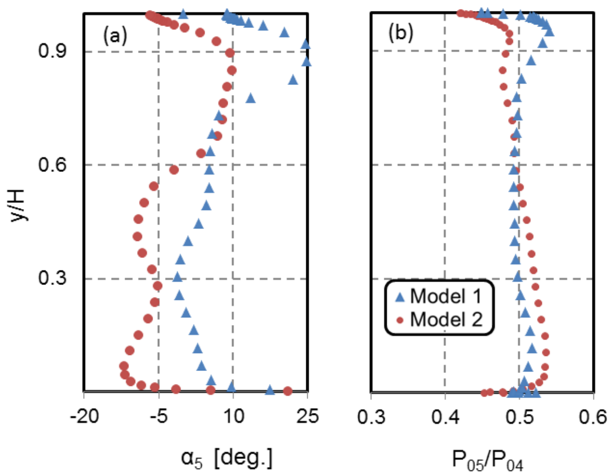

Figure 12. Stage outlet radial distributions a) absolute swirl angle, b) Non-dimensional total pressure

(3) What is the effect of the nozzle since not only the turbines are changed but the nozzles are changed also in the engine tests ?

The authors believe the nozzle has minor effect on the engine perfromance. The both nozzles are designed in such a way that the flow reaches sonic conditions at the outlet area. In the paper we presented Fig. 9 to prove similarity of the aerodynamic performances of both engines. In order to comply with the reviewer comment, a brief nozzle comparison has been described in Numerical Methods/Design Approach section.

(Page 3) "Both designs have their unique exhaust nozzles that have sonic conditions while supplying the designed back-pressure to turbines (see Figure 8). Furthermore, nozzle design has been taken as a part of the turbine-redesigning process and the CFD models include nozzle geometry together with the turbine stage."

(4) Which commercial codes are used for the CFD, Structural and Thermal analysis?

The CFD calculations have been performed by Numeca Fine^{TM}/Turbo 3D RANS based solver. The structrual calculations have been handled by ANSYS. The paper does not involve these to avoid advertisement issues.